Received: 12 April 2022 | Revised: 11 October 2022 | Accepted: 28 October 2022

DOI: 10.1002/term.3365

WILEY

RESEARCH ARTICLE

# Examination of epigenetic inhibitor zebularine in treatment of skin wounds in healthy and diabetic mice

Piotr Sass[1] | Paweł Sosnowski[1] | Jolanta Kamińska[1] | Milena Deptuła[2] | Aneta Skoniecka[2] | Jacek Zieliński[3] | Sylwia Rodziewicz-Motowidło[4] | Michał Pikuła[2] | Paweł Sachadyn[1]

[1]Laboratory for Regenerative Biotechnology, Gdańsk University of Technology, Gdańsk, Poland

[2]Laboratory of Tissue Engineering and Regenerative Medicine, Division of Embryology, Medical University of Gdańsk, Gdańsk, Poland

[3]Department of Oncologic Surgery, Medical University of Gdańsk, Gdańsk, Poland

[4]Department of Biomedicinal Chemistry, Faculty of Chemistry, University of Gdańsk, Gdańsk, Poland

**Correspondence**

Paweł Sachadyn and Piotr Sass, Laboratory for Regenerative Biotechnology, Gdańsk University of Technology, Gdańsk 80-233, Poland.
Email: psach@pg.edu.pl and piotrsass@gmail.com

**Funding information**

Narodowe Centrum Badań i Rozwoju, Grant/Award Number: TECHMATSTRATEG2/410747/11/NCBR/2019

## Abstract

DNA methyltransferase inhibitor zebularine was proven to induce regeneration in the ear pinna in mice. We utilized a dorsal skin wound model to further evaluate this epigenetic inhibitor in wound healing. Full-thickness excisional wounds were made on the dorsum of 2 and 10-month-old healthy BALB/c and 3 and 8-month-old diabetic (db/db) mice, followed by topical or intraperitoneal zebularine delivery. Depending on the strain, age, dose, and delivery, the zebularine treatments either had no effect or accelerated or delayed wound closure. In principle, zebularine applied topically moderately promoted wound closure in the healthy but markedly delayed in the diabetic mice, which was in line with decreased viability of cultured keratinocytes from diabetic patients exposed to zebularine. The histological analysis revealed an improvement in the architecture of restored skin in zebularine-treated mice, manifested as a distinct layered pattern resembling *panniculus carnosus*. The finding corresponds with the zebularine-mediated activation of the *Wnt5a* gene, an essential regulator of Wnt signaling, the pathway involved in hair follicle development, the process which in turn is connected with regenerative skin healing. Although zebularine did not remarkably accelerate wound healing, zebularine and other epigenetic inhibitors deserve further testing as potential drugs to improve the quality of restored skin.

KEYWORDS

DNA methylation, epigenetic drugs, mouse, regeneration, regenerative medicine, skin, wound healing, zebularine

## 1 | INTRODUCTION

The skin is the largest organ in the human body and plays an essential role as a barrier between the organism and the environment. Due to its role, skin damage is widespread. In principle, minor incisional injuries heal rapidly. In contrast, more extensive excisional skin injuries often lead to complications and scarring (Marshall et al., 2018; Nowak et al., 2021), delayed wound healing, in extreme cases, chronic wounds, defined as those that fail to heal within 3 weeks (Martinengo et al., 2019). New pharmacological solutions to improve skin wound healing and prevent scarring are needed. Epigenetic inhibitors appear as interesting candidate drugs owing to their ability to activate genes

essential for the regenerative capacity of cells and tissues (Sass et al., 2019).

An analog of cytidine, pyrimidin-2-one ribonucleoside, called zebularine, is an inhibitor of DNA methyltransferases. Its synthesis was first described in 1961 (Funakoshi et al., 1961). In earlier studies, zebularine was examined as a potential bacteriostatic agent (Oyen et al., 1973), the inhibitor of thymidylate synthase (Votruba et al., 1973), and cytidine deaminase (Kim et al., 1986). Later, the inhibitory effect on DNA methyltransferases was found (Cheng et al., 2003). Zebularine does not bind DNA methyltransferases as a free molecule. Zebularine inhibits DNA methyltransferases after it is incorporated into DNA. This requires metabolic activation, including phosphorylation to diphosphate, reduction to deoxynucleotide, and phosphorylation to 2′-deoxyzebularine-5′-triphosphate (Ben-Kasus et al., 2005), which is integrated into DNA in place of cytidine during replication (Lee et al., 2004). DNA methyltransferase forms a covalent bond with DNA-incorporated zebularine resulting in irreversible inhibition (Zhou et al., 2002) and cellular depletion of this enzyme (Cheng et al., 2004). Zebularine was investigated primarily as an anticancer agent displaying DNA demethylating and cytotoxic effects (Marquez et al., 2005). In contrast to other nucleoside inhibitors of DNA methyltransferases approved as anti-cancer drugs, 5-azacitidine or 5-aza-2-deoxycytidine, zebularine shows minimal toxicity to animals, even at high doses and prolonged treatment. In mice, no toxic effects were observed following oral delivery in drinking water (0.2 mg/ml) for 4 months, seven intraperitoneal injections at 1000 mg/kg within 11 days (Sass et al., 2019), and intraperitoneal injections for 78 consecutive days at 400 mg/kg (Herranz et al., 2006). Notably, as reported by Herranz et al., after the 78-day treatment at 400 mg/kg, careful pathologic studies failed to identify any sign of toxicity in any organ or tissue.

Our previous work demonstrated a new epigenetic strategy for tissue regeneration based on zebularine. Zebularine induced global and gene-specific demethylation in the mouse ear pinna wounds that correlated with greatly improved healing. Methylation of gene promoter regions is connected with gene silencing. Zebularine-mediated demethylation was associated with transcriptional activation of genes essential in regeneration, such as pluripotency factors and neurotrophins. Further, we found that retinoic acid potentiated zebularine action, resulting in complete ear hole closure, which was spectacular, as, in most laboratory mice, through-and-through holes in ear pinnae display only partial closure (Sass et al., 2019). The result supported our previous findings on the epigenetic basis of regenerative potential (Górnikiewicz et al., 2013, 2016, 2017; Podolak-Popinigis et al., 2016).

In the present study, we investigate the effectiveness of zebularine in dorsal skin injury in healthy 2 and 10-month-old mice and explore the potential use of epigenetic strategy in promoting wound healing. In addition, we examine zebularine activity in a model of diabetic mice with a defective leptin receptor gene exhibiting severely delayed healing (Michaels et al., 2007).

## 2 | MATERIALS AND METHODS

### 2.1 | Laboratory animals

BALB/c mice were obtained from the Tri-City Academic Laboratory Animal Center, BKS.Cg-Dock7$^{m}$ +/+ Lepr$^{db}$/J (db/db) mice were obtained from Charles Rivers Laboratories. Experiments were performed on females. The size of tested groups, mouse age and strains are detailed in Table 1. All animal procedures were approved by the Local Ethics Committee in Bydgoszcz (approval no. 49/2016).

### 2.2 | Dorsal skin injury

Prior to the experiment, mice were anesthetized with isoflurane. Mouse dorsal skin was shaved and disinfected. The skin was gathered into a fold, running parallel to the spine. Then the mouse was laid on the side, and the fold was pierced with a 6 mm biopsy punch to create two symmetrical circular wounds on the dorsum (Figure 1). Wounds were then covered with transparent Tegaderm film, and the torso of the mouse was wrapped in an adhesive plaster. The dressing was changed daily during the first and every other day during the second week post-injury.

In two groups, the animals had silicone rings attached to the skin around the wound according to the protocol provided by Wang et al. (2013). The procedure was carried out as stated above with indicated modifications. Before wounds were covered with Tegaderm, silicone ring wound splints (Grace Bio-Labs Cat. No. GBLRD476687 with suture sites: 14 mm - outer diameter, 7 mm - inner diameter, 0.5 mm - thickness) were attached with cyanoacrylate glue and sutured to the skin so that the wound was in the center of the ring (Figure 1).

Glucose was measured weekly in blood from the tail vein to confirm hyperglycaemia in db/db mice. All animals with blood glucose above 250 mg/dl were considered diabetic.

### 2.3 | Zebularine application

Zebularine (Tokyo Chemical Industries, Cat. No. Z0022) was dissolved in saline and stored frozen at −20°C. Before the application, the zebularine solution was thawed and heated to 37°C. After the injury and prior to zebularine delivery, the animals were randomly divided into treatment and control groups. Zebularine was administered as saline solutions (0.9% NaCl) either intraperitoneally (i.p.) or topically. For i.p. injections, a solution of either 50 or 25 mg/ml of zebularine was injected at a volume of 20 µl/g b.m. (body mass), which translates to a dose of 1000 or 500 mg/kg b.m., respectively. Injections were performed for five consecutive days from the day of the injury (day 0) and on days 7 and 10 after the injury (Figure 2a). For topical administration, 10 µl of either 50 or 200 mg/ml of zebularine in saline was applied to each wound for five consecutive days after the injury (Figure 2b). Of note, we observed that 10 µl

**TABLE 1** Description of experimental animals

| Strain | Experiment | Initial age | Number |
|---|---|---|---|
| BALB/c (healthy mice) | Zebularine 500 mg/kg b.m. i.p. | 8–10 weeks | 6 |
| | Zebularine 1000 mg/kg b.m. i.p. | 8–10 weeks | 6 |
| | Saline topical | 8–10 weeks | 18 |
| | Zebularine 0.5 mg per wound[a] topical | 8–10 weeks | 6 |
| | Zebularine 2.0 mg per wound[b] topical | 8–10 weeks | 12 |
| | Saline topical | 10 months | 12 |
| | Zebularine 0.5 mg per wound[a] topical | 10 months | 6 |
| | Zebularine 2.0 mg per wound[b] topical | 10 months | 6 |
| | Saline topical, splinted | 8–10 weeks | 5 |
| | Zebularine 0.5 mg per wound[a] topical, splinted | 8–10 weeks | 5 |
| | Zebularine 500 mg/kg b.m., RA 8 mg/kg b.m. i.p. | 8–10 weeks | 6 |
| BKS.Cg-Dock7$^{m}$ +/+ Lepr$^{db}$/J (diabetic mice db/db) | Saline topical | 12 weeks | 6 |
| | Zebularine 0.5 mg per wound[a] topical | 12 weeks | 6 |
| | Saline topical | 8 months | 6 |
| | Zebularine 0.5 mg per wound[a] topical | 8 months | 6 |

Abbreviations: b.m., body mass; i.p., intraperitoneal.

[a]Stock concentration 50 mg/ml.

[b]Stock concentration 200 mg/ml.

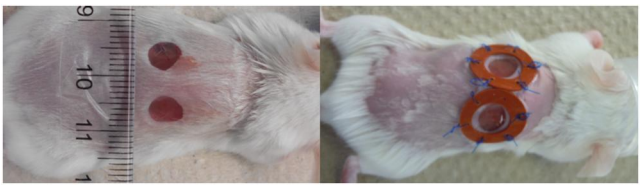

**FIGURE 1** Representative images of mice after wounding. Unsplinted dorsal skin wounds—left; splinted skin wounds—right.

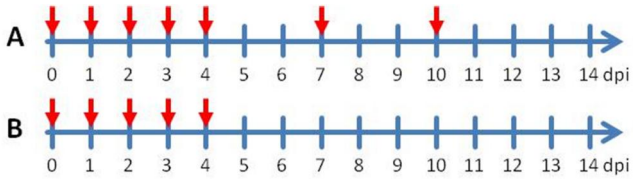


**FIGURE 2** Zebularine application schedules. Red arrows indicate the days on which zebularine was administered. (a) Intraperitoneal administration. (b) Topical administration

droplets applied topically absorbed immediately in 6-mm wounds. Animals from the control groups received saline in adequate volumes.

## 2.4 | Retinoic acid application

All-trans-retinoic acid (Tokyo Chemical Industries, Cat. No. R0064) dissolved in rape seed oil (1 mg/ml) was injected intraperitoneally (8 mg/kg b.m.) on days 0, 2, 4, 7, 9, and 11 post-injury.

## 2.5 | Wound closure measurement

Wounds were photographed on days 0, 2, 4, 7, 9, 11, and 14 after the injury with a ruler placed adjacent to them. Wound areas directly after the injury ($S_0$) and at subsequent time points ($S_i$) were determined using the image analysis software ImageJ (Schneider et al., 2012). Wound closure ($C_i$) was calculated according to the formula given below.

$$C_i = (S_0 - S_i)/S_0$$

## 2.6 | Histological sample preparation

Mice were sacrificed on day 18 of the experiment. Dorsal skin was sampled and placed in 10% PBS-buffered formalin (pH = 7.4) for at least 2 weeks for fixation. The samples were then embedded in paraffin and cut into 5 μm sections. Skin samples were then stained with Masson's trichrome. The stain yields the following results: epidermis - gray, *stratum corneum* - red or dark red, dermis (collagen) - green, muscle - dark green, sebaceous glands - light gray, nuclei - dark gray.

## 2.7 | Collagen density, blood vessels and hair follicles quantitation

The assessment of collagen density within the wound area was performed from the images of histological tissue sections stained with

Masson's trichrome using the color deconvolution method for ImageJ. Hair follicles and blood vessels in newly formed tissue were quantified as an average number of occurrences per square mm. The results were presented as mean values for 7–9 photographs representing 2–3 mice.

## 2.8 | Measurement of epidermis and dermis thickness

Epidermis and dermis thickness was performed using ImageJ. The thickness was measured in randomly selected areas within the wound area from several (3–5) images. Results were averaged and used to calculate mean epidermis/dermis thickness.

## 2.9 | Transcript levels

Prior to tissue collection, the animals were euthanized in a $CO_2$ chamber. The tissue surrounding dorsal skin wounds was excised with a 4 mm biopsy punch. Tissue samples were preserved in RNAlater (Qiagen) and stored at −80°C. RNA was extracted using an RNeasy Kit (Qiagen). cDNA synthesis was performed in a reaction mix containing 200 ng of RNA, 1 µl of oligo dT20 (100 µM), 1 µl of dNTP mix (10 mM each), 4 µl of 5× reaction buffer (250 mM Tris-HCl, 375 mM KCl, 15 mM $MgCl_2$, 50 mM DTT), and 200 units of Maxima Reverse Transcriptase (Thermo Scientific Bio, Cat. No. EP0742) in a final volume of 20 µl. Real-time PCR was carried out in a final volume of 10 µl containing 5 µl of FastStart Essential DNA Green Master (Roche, Cat. No. 06402712001), 2 µl of cDNA, and 0.25 µl each of forward and reverse primers (10 µM) on a LightCycler LC96 (Roche).PCR was performed in triplicate. The transcript levels were calculated using the $2-\Delta\Delta Ct$ method relative to *Actb* and *Tbp* transcript levels. The primer sequences are listed in Table 2. The qPCR thermal profile was as follows: preliminary denaturation at 95°C for 10 min, followed by 40 cycles consisting of denaturation at 95°C for 10 s, annealing at 70°C for 10 s with touch-down every 1.0°C per cycle, and primer extension at 72°C for 10 s, followed by a final extension at 72°C for 10 min.

## 2.10 | Isolation of skin cells

Skin samples were obtained from patients diagnosed with diabetes in the Surgical Oncology Clinic at the Medical University of Gdańsk and the General Surgery Department with the Oncological Surgery Sub-Department at the Hospital in Koszalin (Table 3). The procedure was approved by the Independent Bioethics Commission for Research of the Medical University of Gdansk (NKBBN/672/2019, NKBBN/670/2019). The skin was cut into small pieces and digested with dispase (Corning, Cat. No. 354235) according to the procedure described before by Langa et al. (2018). After digestion, the epidermis was separated from the dermis with sterile tweezers. Keratinocytes were isolated from the epidermis by two stem trypsin-EDTA (Sigma Aldrich, Cat. No. T4049) digestion. The cells were centrifuged, counted and grown in collagen IV coated Petri dishes (Corning) in EpiLife (Gibco, Cat. No. MEPI500CA) medium supplemented with EpiLife™ Defined Growth Supplement (EDGS) (Gibco, Cat. No. S0125) and 100 U/ml of penicillin, and 100 µg/ml streptomycin (Sigma Aldrich) until the first passage. Fibroblasts were isolated from the dermis with the explant method previously described (Sawicka et al., 2020). The samples of the dermis were placed in culture plates in DMEM HG medium (Sigma Aldrich, Cat. No. D6429) containing 10% of FBS (Sigma Aldrich, Cat. No. F9665) and 100 U/ml of penicillin and 100 µg/ml streptomycin (Sigma Aldrich) in standard conditions (5% $CO_2$, 37°C). After the fibroblasts had grown out from the dermis, the dermis pieces were removed. Then the cells were passaged and grown until the experiments.

**TABLE 3** Characteristics of diabetic patients who were the donors of skin samples

| Patient | Sex | Age | Expanded cell type |
|---|---|---|---|
| Donor 1 | Female | 79 | Fibroblasts |
| Donor 2 | Female | 90 | Fibroblasts |
| Donor 3 | Male | 72 | Fibroblasts |
| Donor 4 | Female | 84 | Keratinocytes |
| Donor 5 | Female | 81 | Keratinocytes |

**TABLE 2** List of PCR primer sequences

| Gene name | Forward primer sequence | Reverse primer sequence |
|---|---|---|
| *Krt17* | CGCTTATTACCATACCATTGAGG | TTGGTACGGAAGTCATCGGC |
| *Lef1* | TGAGTGCACGCTAAAGGAGA | ATAATTGTCTCGCGCTGACC |
| *Pou5f1* | GGAGAAGTGGGTGGAGGAAG | TGATTGGCGATGTGAGTGAT |
| *Wnt5a* | AATGAAGCAGGCCGTAGGA | AGCCAGCACGTCTTGAGG |
| *Actb* | GGCTGTATTCCCCTCCATCG | CCAGTTGGTAACAATGCCATGT |
| *Tbp* | GAGAGCCACGGACAACTGCG | GGGAACTTCACATCACAGCTC |

### 2.11 | Analysis of cell viability

The analysis of cell viability after the stimulation with zebularine was performed with an XTT assay (Sigma Aldrich, Cat. No. 1146501 5001). Fibroblasts (in the fifth passage) were seeded into 96-well dishes (5000 per well) in a DMEM HG medium supplemented with 10% FBS. After 24 h, the cells were washed twice, and the medium was exchanged for serum-free DMEM. Then, the cells were stimulated with appropriate concentrations of zebularine. Human keratinocytes (in the second or third passage) were seeded in 48-well plates (20,000 per well) in Epilife medium supplemented with EDGS and 10% FBS. After 24 h, the medium was exchanged for a serum-free Epilife with EDGS. Cells were grown in plates for an additional 48 h when the medium was changed again for serum and EDGS-free Epilife, and the stimulation with appropriate concentrations of zebularine was performed. For both cell types, after 48 h of incubation, half of the medium was changed to a fresh one, and the second stimulation was performed. After an additional 24 h of incubation, the cell viability XTT assay was done according to the manufacturer's instructions as described before (Deptuła et al., 2020). Cell viability was normalized to the controls (untreated cells). The assays were performed in four experiments for each patient and condition.

### 2.12 | Statistical analysis

Wound closure, gene expression, and adnexa counting results were tested for statistical significance using the two-tailed Mann-Whitney test. Cell culture results were analyzed using an ANOVA mixed model followed by pairwise comparisons with Tukey's test. All calculations were computed using XLSTAT (Addinsoft). Statistical significance was marked as follows: $^{*}p < 0.05$, $^{**}p < 0.01$, $^{***}p < 0.001$.

## 3 | RESULTS

### 3.1 | Zebularine in the healing of skin wounds

To examine whether zebularine can aid in healing skin injury, we tested intraperitoneal injections of zebularine in BALB/c mice. This experiment replicated the protocol effective in ear pinna regeneration used in our previous studies (Sass et al., 2019). The measurement of wound closure showed a significant delay in healing in the group receiving 1000 mg/kg b.m. (body mass) of zebularine and no difference in the group receiving 500 mg/kg b.m. (Figure 3a). Also, combined intraperitoneal delivery of zebularine and retinoic acid, found in our previous research to induce complete ear pinna hole closure (Sass et al., 2019), did not accelerate dorsal skin wound healing (Figure 3b).

Next, we tested the topical application to dorsal skin wounds with zebularine concentrations of 50 and 200 mg/ml, corresponding to 0.5 and 2.0 mg per wound, respectively (Figure 2b). Following the topical treatment, a less substantial delay in wound healing was observed than for intraperitoneally administered zebularine; however, the delay was determined for both the lower and higher concentrations. A modest but statistically significant improvement in wound closure was recorded on day 14 in the group treated topically with 200 mg/ml of zebularine (Figure 3c).

Next, we evaluated zebularine therapy in middle-aged mice. In 10-month-old BALB/c mice, topical application of 50 mg/ml zebularine caused a moderate, yet statistically significant, increase in skin wound closure up to the seventh day of the experiment (Figure 3d). Also, we observed a slight but statistically insignificant increase in the animals treated with 200 mg/ml of zebularine. From day 9 until the end of the experiment, no differences were observed in wound closure in both zebularine-treated groups.

We also applied a wound splinting model where silicone rings are attached to the wound edges to prevent contraction and distortion. The results in the groups with splinted wounds were the most consistent; however, we did not observe differences in wound closure between the zebularine and saline-treated mice (Figure 3e).

Further, we conducted experiments using a model of impaired skin healing in type 2 diabetic mice (db/db). We used mice of 3 months of age at the early onset of diabetes and 8-month-old ones representing severe diabetes. Here the results were in line with the initial experiments in healthy mice, and a significant decrease in wound closure was visible from day 7 onwards in both younger and older mice (Figure 3f,g). In all cases where we observed the delay in wound healing, it occurred around days 9 and 11 after the injury, a few days after the zebularine administration ceased (Figure 2b).

### 3.2 | Zebularine effect on skin architecture

To evaluate the quality of restored skin, we prepared histological sections of dorsal skin samples collected on day 18 post-injury and stained them with Masson's trichrome. As demonstrated in Figure 4, neither group showed well-developed skin architecture. We measured the density of hair follicles and blood vessels in zebularine and saline-treated skin samples and determined no statistically significant differences (Figure 5). We also analyzed collagen density in zebularine-treated samples and compared them to control samples. As before, no statistically significant differences were found (Figure 5). Also, the epidermis and dermis thickness measurements in zebularine-treated samples revealed no differences between zebularine-treated and control skin (Figure 5).

While typical indicators of skin wound healing, hair follicles, blood vessels, and collagen density analyzed in histological images showed no quantitative change following zebularine treatment, we found a structural difference. The deeper layers of the wound area in the zebularine-treated samples showed a distinct layered pattern that was not recognized in the control samples. This observation might suggest the development of *panniculus carnosus*, a thin (approximately 0.2 mm in dorsal skin in mice) layer of striated muscles between the dermis and *fascia* (Naldaiz-Gastesi et al., 2018), in zebularine-treated skin (Figure 4). Figure S1 presents more examples of the structure identified in zebularine-treated mice.

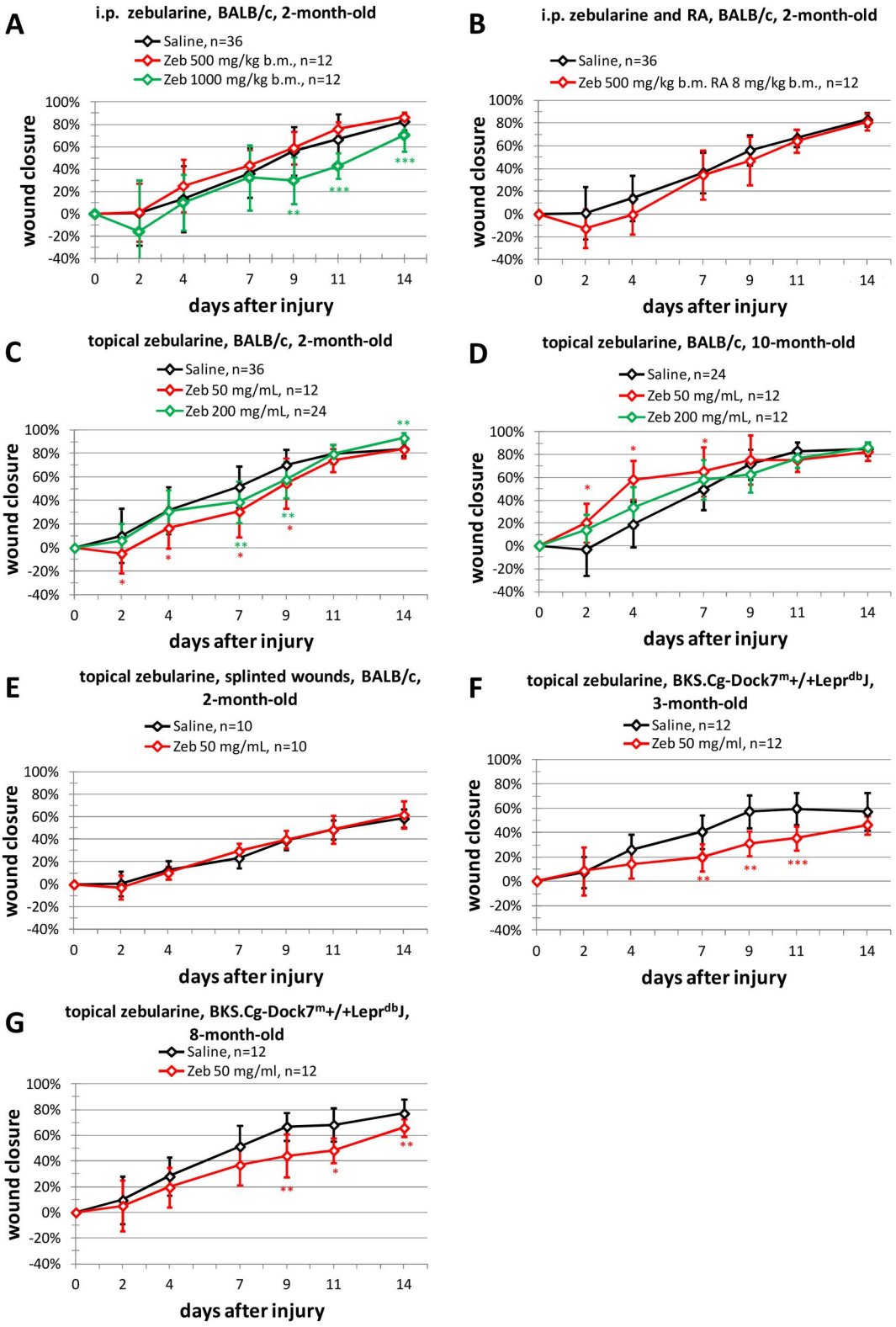


**FIGURE 3** Closure of wounds in dorsal skin: (a) BALB/c mice, 2-month-old, i.p. administered Zeb; (b) BALB/c mice, 2-month-old, i.p. delivered Zeb and RA; (c) BALB/c mice, 2-month-old, topically administered Zeb, mice; (d) BALB/c mice, 10-month-old, topically administered Zeb; (e) BALB/c mice, 2-month-old, splinted wounds, topically administered Zeb; (f) diabetic mice, 3-month-old, topically administered Zeb; and (g) diabetic mice, 8-month-old, topically administered Zeb. Sample size (*n*) represents the number of wounds. i.p., intraperitoneally; RA, retinoic acid; Zeb, zebularine. $^{*}p < 0.05$, $^{**}p < 0.01$, $^{***}p < 0.001$

### 3.3 | Transcriptional responses of genes involved in hair follicle neogenesis

Hair follicle neogenesis genes are characteristic of embryonic development and have shown activation after excisional injury in regenerating skin (Ito et al., 2007). Wnt signaling and cellular pluripotency are essential in skin regeneration processes. Transcriptional profiling in healing skin revealed the induction of *Wnt5a*, a non-canonical regulator of Wnt, the signaling involved in hair follicle morphogenesis (Reddy et al., 2001), *Krt17*, a hair follicle differentiation marker (McGowan & Coulombe, 1998), *Lef1*, active in developing skin fibroblasts and *Pouf5f1*, known as *Oct4*, a critical pluripotency factor. The expression levels of *Krt17* and *Lef1* were elevated in both zebularine and saline-treated controls compared to uninjured and untreated skin on days 10 and 15 post-injury (Figure 6). The *Pou5f1* gene was significantly induced on day 10 post-injury in zebularine, but not saline-treated skin relative to uninjured and untreated skin. Induction of *Pouf5f1* on day 15 after zebularine treatment, although noticeably higher compared to day 0, did not reach statistical significance. However, the differences between the zebularine-treated mice and the parallel controls were not significant. In the case of *Wnt5a*, a significant induction on day 10 post-injury was determined in the zebularine-treated but not in the control skin (Figure 6).

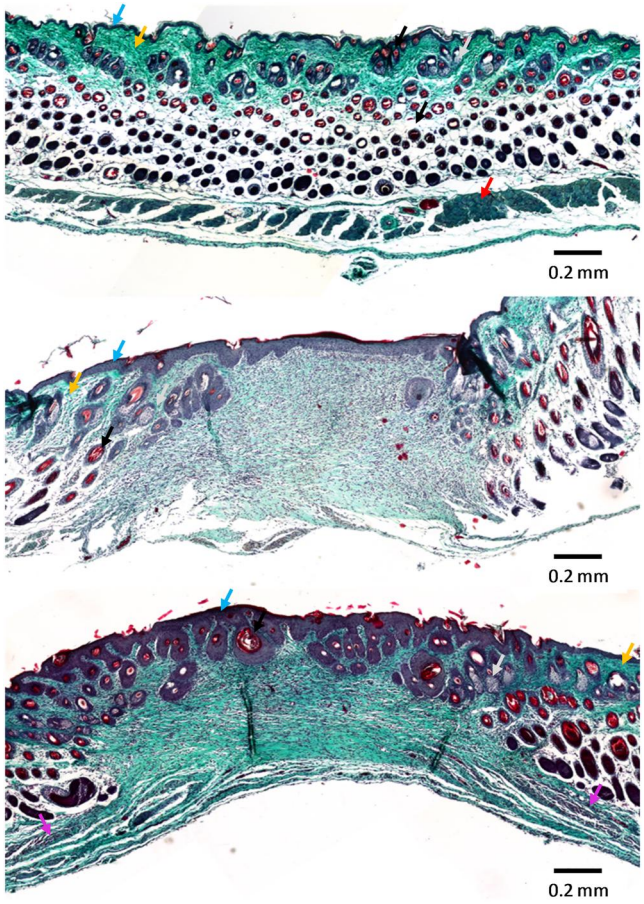


**FIGURE 4** Representative images of dorsal skin sections from skin treated with 200 mg/ml of zebularine (bottom panel) and the controls of uninjured skin (top panel) and saline-treated injured skin (middle panel) collected on day 18 post-injury and stained with Masson's trichrome. Arrows indicate epidermis—blue, dermis—yellow, hair follicle—black, sebaceous glands—gray, *panniculus carnosus* in the intact skin—red (top panel), the structure resembling *panniculus carnosus* in the zebularine-treated skin—purple (bottom panel).

### 3.4 | Zebularine effect on the viability of primary fibroblast and keratinocyte cells from diabetic patients

The effect of zebularine was evaluated on the cellular level in cultured keratinocytes, and fibroblasts expanded from skin samples collected from diabetic patients (Table 3). Our previous research on the 46BR.1N fibroblast and the HaCaT keratinocytes tested cells' viability in a wide range of zebularine concentrations from 0.10 to 150 μg/ml (Sass et al., 2019). Due to limited amounts of the expanded cells, we focused on three concentrations of 0.1, 1.0, and 10 μg/ml in the present study. While no decreases in cell viability were determined in the zebularine concentrations of 0.1–10 μg/ml in the fibroblasts, moderate to significant inhibition was observed in the keratinocytes (Figure 7).

## 4 | DISCUSSION

Our previous success in promoting tissue regeneration in the mouse ear pinna with zebularine (Sass et al., 2019) and the current failure to replicate the effect in dorsal skin might be due to the inherent differences in the repair models. First, in contrast to the dorsum, the dermis is supported by the cartilage layer in the ear pinna.

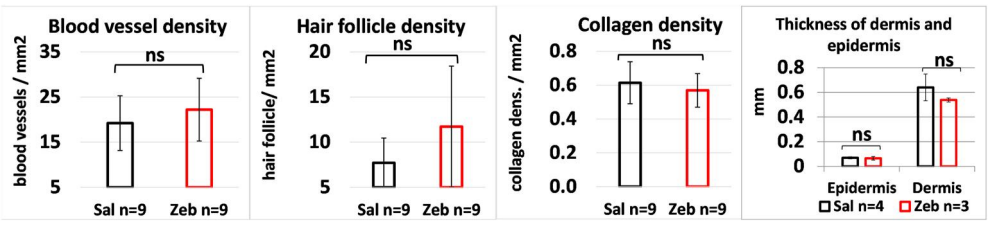


**FIGURE 5** Evaluation of collagen, blood vessel and hair follicles density, the thickness of dermis and epidermis in zebularine (topical application, 200 mg/ml) and saline-treated wounds on day 18 post-injury. The error bars represent SD; *n* is the number of wounds.

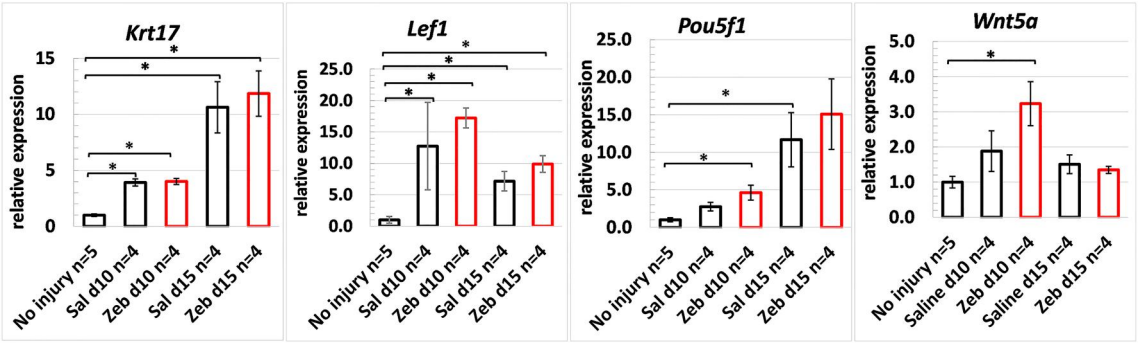


**FIGURE 6** Expression changes of genes involved in hair follicle neogenesis in healing dorsal mouse skin in response to topical zebularine treatment on days 10 and 15 after the injury. The error bars represent SEM. Relative expression was normalized to that in uninjured skin. $^{*}p < 0.05$

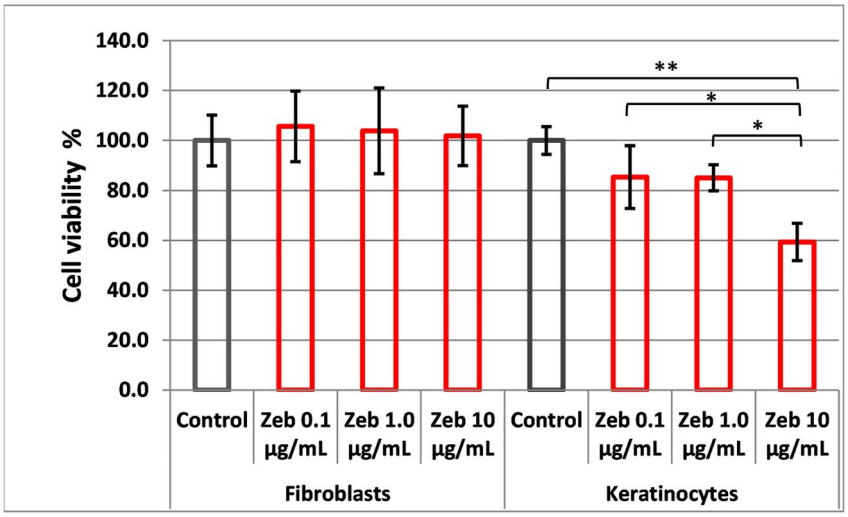


**FIGURE 7** Viability of primary human cells expanded from diabetic patients' skin after 72-h exposure to zebularine. The results represent means from four replicates for three fibroblasts and two keratinocytes donors. The error bars represent SD. The results were normalized to the control cells. The *p*-values determined in pairwise comparisons were as follows: Fibroblasts: Control versus 10.0–0.924, Control versus 1.0–0.974, Control versus 0.1–0.997, 0.1 versus 10–0.974, 0.1 versus 1.0–0.996, 1.0 versus 10.0–0.997; Keratinocytes: Control versus 10.0–0.009, Control versus 1.0–0.193, Control versus 0.1–0.204, 0.1 versus 10–0.043, 0.1 versus 1.0–1.000, 1.0 versus 10.0–0.045. $^{*}p < 0.05$, $^{**}p < 0.01$,

Noteworthy, the cartilage growth advances with the growth of skin (Sass et al., 2019), although, in the MRL mouse, further cartilage reconstruction was observed after ear pinna hole closure (Clark et al., 1998). Second, to seal the injury, dorsal skin has to cover the whole wound area, whereas, in the ear pinna, it is enough that the skin secures the wound margins. Third, contraction is a major component of skin wound healing in rodents (Chen et al., 2015). In the case of ear pinna regeneration, the primary source of healing is observed in tissue growth that fills the wound area (Clark et al., 1998; Seifert et al., 2012; Williams-Boyce & Daniel Jr, 1980). Fourth, the essential difference between the models is that 6-mm excisional wounds in murine dorsal skin heal without any treatment, whereas 2-mm ear pinna punch holes in most strains of laboratory mice remain for life. In the dorsal skin model, treatment is intended to accelerate wound closure which is to occur in any case. In the ear pinna, successful treatment has to break some endogenous limitations to induce ear hole closure. In principle, our data for the dorsal skin show that independent of initial improvements observed up to day 9 post-injury, zebularine-treated and control wounds tend to achieve similar closure by day 14.

Interestingly, topical treatment of 10-month-old mice with zebularine at the lower concentration applied, 50 mg/ml, seems to accelerate skin wound closure during the early days after injury. The observation may correspond with the findings by Reines et al., who showed that 8-month-old C57BL/6 and BALB/c mice could close ear punch wounds better than 2-month-old animals (Reines et al., 2009).

No effect of zebularine in splinted dorsal skin injuries is somewhat concerning. On the one hand, the wound area measurement

seems more reliable in the splinted model than in the unsplinted one. However, in the unsplinted wounds, we observed a delay in wound healing after zebularine delivery absent in the splinted ones. This provokes a question of whether the attachment of silicone rings impairs skin healing to such an extent that minor effects produced by the tested therapy might not be observable.

Although zebularine did not accelerate mouse dorsal skin wound closure markedly in most cases, an improvement in tissue architecture was observed in zebularine-treated skin. While no differences in the blood vessel or hair follicle density were determined, we saw a layered pattern in the deeper areas of the injury, suggesting a restoration of *panniculus carnosus* (Figure 4). Unlike most mammals, *panniculus carnosus*, considered vestigial in humans (Naldaiz-Gastesi et al., 2018), is mostly absent except for some facial areas, including eyebrows, eyelids, nose, lips, and chin (Yus & Simón, 2000). A recent report demonstrates the presence of *panniculus carnosus* at the heel and provides evidence indicating that impaired restoration of *panniculus carnosus* can be critical for the chronicity of heel pressure ulcers (Nasir et al., 2022). This observation signals that methods promoting *panniculus carnous* restoration in animal models may have vital implications for wound healing in humans. Of note, *panniculus carnosus* was proposed as a model of striated muscle regeneration (Bahri et al., 2019).

As hair follicle neogenesis is connected with regenerative skin healing (Ito et al., 2007), we examined the activity of genes involved in this process. Transcriptional activation of the *Wnt5a* gene, one of the regulators of hair follicle growth (Reddy et al., 2001), was determined following zebularine treatment. As shown in cellular (Ben-Kasus et al., 2005) and animal models (Herranz et al., 2006), zebularine exerts minimal toxicity, especially when compared to other nucleoside inhibitors of DNA methyltransferases like 5′-azacitidine. In our previous study, we evaluated the effects of zebularine on immortalized keratinocyte (HaCaT) and fibroblast (46BR.1N) cell lines. The analyses showed both inhibitory and pro-proliferative effects, dependent on the concentration (Sass et al., 2019). Specifically, after 72 h, 46BR.1N cells demonstrated a significant increase at 0.1 μg/ml and a marked decrease in viability at 10 μg/ml of zebularine, whereas the HaCaT cells displayed no effect at these concentrations. The concentration of 1.0 μg/ml had no impact on the 46BR.1N cells and markedly induced the viability of the HaCaT cells. The observations in the immortalized cell lines are not consistent with the present study results, where the same zebularine concentrations had no impact on the viability of fibroblasts. Zebularine had an inhibitory effect on the keratinocytes expanded from the skin of diabetic patients, which increased with the concentration. This decreased viability of keratinocytes expanded from diabetic patients (Figure 7) is in line with the delayed skin wound closure in diabetic mice (Figure 3f,g). It is worth noting that at moderate concentrations, zebularine appears safe for the skin cells, although in the case of the cell lines expanded from diabetic patients, the keratinocytes were more sensitive than the fibroblasts. It is worth noting that the diabetic cells represented aged patients.

Notably, as shown in the ear pinna model, zebularine treatment retarded the hole closure for the initial 2 weeks (Sass et al., 2019). The observations suggest that zebularine treatment of skin wounds may require careful dose-tuning. However, in the case of zebularine, such dose optimization may be challenging to achieve, as the compound is susceptible to rapid conversion to uridine by cellular aldehyde oxidases (Ben-Kasus et al., 2005). In addition, zebularine has been reported to cause DNA mutations in bacterial cells (Lee et al., 2004) and DNA breaks in the XRCC1 hamster ovarian cells deficient in single-strand break repair (Orta et al., 2017). Accordingly, finding a balance between cytotoxicity and biodegradation may be necessary.

Zebularine treatment delineated an epigenetic strategy for regeneration in the ear pinna model (Sass et al., 2019). Zebularine-mediated induction of tissue regeneration in the ear pinna demonstrated that using an epigenetic inhibitor might promote a regenerative response. More small-molecule epigenetic inhibitors are becoming available for research (Ganesan et al., 2019), and the chances of identifying novel epidrugs displaying better pharmacological properties than zebularine are increasing. In the case of the dorsal skin, using another DNA methyltransferase inhibitor, displaying better stability, lower cytotoxicity and not causing DNA damage might be a better strategy for promoting wound healing. On the other hand, despite its toxicity, zebularine may be safe, especially for topical use. Of note, owing to its mechanism of action dependent on incorporation to DNA, zebularine is expected to act on proliferating cells mainly, and such are found in healing wounds. For the same reason, zebularine appears unharmful to non-proliferating cells. What is important, the products of zebularine bioconversion, like uridine, are endogenous compounds (Beumer et al., 2006).

## 5 | CONCLUSIONS

Following the same treatment schedule, zebularine previously proved to induce ear pinna regeneration failed to accelerate dorsal skin wound healing in mice markedly. Nevertheless, the structure resembling *panniculus carnosus* identified in the zebularine-treated but not in the control wounds indicates that zebularine may improve the architecture of the restored tissues. The results suggest two directions to developing regenerative skin therapies using DNA demethylating agents. One possibility is optimizing dosage and trying zebularine further for anti-scarring applications. Another solution is testing other DNA demethylating agents as candidate drugs for wound treatment.

### AUTHOR CONTRIBUTIONS

Conceptualisation: Paweł Sachadyn, Piotr Sass, Paweł Sosnowski. Methodology: Piotr Sass, Paweł Sosnowski, Jolanta Kamińska. Investigation: Piotr Sass, Paweł Sosnowski, Jolanta Kamińska, Milena Deptuła, Aneta Skoniecka, Jacek Zieliński. Writing—original draft preparation: Piotr Sass. Writing—review and editing: Paweł

Sachadyn. Project supervision and manuscript revision: Paweł Sachadyn, Michał Pikuła, Sylwia Rodziewicz-Motowidło. Funding acquisition: Paweł Sachadyn, Sylwia Rodziewicz-Motowidło, Michał Pikuła. Resources: Jacek Zieliński. Formal analysis: Paweł Sachadyn. All authors have read and agreed to the published version of the manuscript.

## ACKNOWLEDGMENTS

This study was supported by the grant "BIONANOVA" of the National Center for Research and Development of Poland No. TECHMATSTRATEG2/410747/11/NCBR/2019. The presented research was also supported in part by the grant "Drug candidate for wound healing" under the project Incubator of Innovation+—"Support for management of scientific research and commercialization of R&D results in scientific units and enterprises," implemented under the Intelligent Development Operational Program 2014–2020 (Action 4.4) awarded to Dr. Sachadyn. We also thank for the support from the BioVentures Institute Foundation, Gdańsk, Poland. The funding source had no role in the writing of the manuscript or in the decision to submit it for publication. We would like to acknowledge the support from Dr. Grażyna Peszyńska-Sularz from the Tri-City Academic Laboratory Animal Center, the Medical University of Gdańsk, for her help in the preparation of the application to the Local Ethics Committee in Bydgoszcz. We also acknowledge the support of Anna Żyłko, Beata Muszyńska DVM, Agnieszka Jakubiak and Monika Dmochowska from the Tri-City Academic Laboratory Animal Center, the Medical University of Gdańsk in animal handling and performance of the surgeries. We want to acknowledge the help of Ewa Nowicka from the Department of Clinical Anatomy at the Medical University of Gdańsk in the preparation of histological samples.

## CONFLICT OF INTEREST

The authors declare no conflict of interest.

## DATA AVAILABILITY STATEMENT

The data that support the findings of this study are available from the corresponding author upon reasonable request.

## ORCID

*Piotr Sass* https://orcid.org/0000-0002-1199-8203
*Milena Deptuła* https://orcid.org/0000-0003-4875-770X
*Michał Pikuła* https://orcid.org/0000-0001-7751-9781
*Paweł Sachadyn* https://orcid.org/0000-0002-5087-844X

## REFERENCES

Bahri, O. A., Naldaiz-Gastesi, N., Kennedy, D. C., Wheatley, A. M., Izeta, A., & McCullagh, K. J. (2019). The panniculus carnosus muscle: A novel model of striated muscle regeneration that exhibits sex differences in the mdx mouse. *Scientific Reports*, *9*(1), 1–15. https://doi.org/10.1038/s41598-019-52071-2

Ben-Kasus, T., Ben-Zvi, Z., Marquez, V. E., Kelley, J. A., & Agbaria, R. (2005). Metabolic activation of zebularine, a novel DNA methylation inhibitor, in human bladder carcinoma cells. *Biochemical Pharmacology*, *70*(1), 121–133. https://doi.org/10.1016/j.bcp.2005.04.010

Beumer, J. H., Joseph, E., Egorin, M. J., Parker, R. S., D'argenio, D. Z., Covey, J. M., & Eiseman, J. L. (2006). A mass balance and disposition study of the DNA methyltransferase inhibitor zebularine (NSC 309132) and three of its metabolites in mice. *Clinical Cancer Research*, *12*(19), 5826–5833. https://doi.org/10.1158/1078-0432.ccr-06-1234

Chen, L., Mirza, R., Kwon, Y., DiPietro, L. A., & Koh, T. J. (2015). The murine excisional wound model: Contraction revisited. *Wound Repair and Regeneration*, *23*(6), 874–877. https://doi.org/10.1111/wrr.12338

Cheng, J. C., Matsen, C. B., Gonzales, F. A., Ye, W., Greer, S., Marquez, V. E., Jones, P. A., & Selker, E. U. (2003). Inhibition of DNA methylation and reactivation of silenced genes by zebularine. *Journal of the National Cancer Institute*, *95*(5), 399–409. https://doi.org/10.1093/jnci/95.5.399

Cheng, J. C., Yoo, C. B., Weisenberger, D. J., Chuang, J., Wozniak, C., Liang, G., Marquez, V. E., Greer, S., Orntoft, T. F., Jones, P. A., & Thykjaer, T. (2004). Preferential response of cancer cells to zebularine. *Cancer Cell*, *6*(2), 151–158. https://doi.org/10.1016/j.ccr.2004.06.023

Clark, L. D., Clark, R. K., & Heber-Katz, E. (1998). A new murine model for mammalian wound repair and regeneration. *Clinical Immunology and Immunopathology*, *88*(1), 35–45. https://doi.org/10.1006/clin.1998.4519

Deptuła, M., Karpowicz, P., Wardowska, A., Sass, P., Sosnowski, P., Mieczkowska, A., Filipowicz, N., Dzierzynska, M., Sawicka, J., Langa, P., Schumacher, A., Cichorek, M., Zielinski, J., Kondej, K., Kasprzykowski, F., Czupryn, A., Janus, L., Mucha, P., & Nowicka, E. (2020). Development of a peptide derived from platelet-derived growth factor (PDGF-BB) into a potential drug candidate for the treatment of wounds. *Advances in Wound Care*, *9*(12), 657–675. https://doi.org/10.1089/wound.2019.1051

Funakoshi, R., Irie, M., & Ukita, T. (1961). Syntheses of unnatural pyrimidine nucleosides. *Chemical and Pharmaceutical Bulletin*, *9*(5), 406–408. https://doi.org/10.1248/cpb.9.406

Ganesan, A., Arimondo, P. B., Rots, M. G., Jeronimo, C., & Berdasco, M. (2019). The timeline of epigenetic drug discovery: From reality to dreams. *Clinical Epigenetics*, *11*(1), 1–17. https://doi.org/10.1186/s13148-019-0776-0

Górnikiewicz, B., Ronowicz, A., Krzemiński, M., & Sachadyn, P. (2016). Changes in gene methylation patterns in neonatal murine hearts: Implications for the regenerative potential. *BMC Genomics*, *17*(1), 1–15. https://doi.org/10.1186/s12864-016-2545-1

Górnikiewicz, B., Ronowicz, A., Madanecki, P., & Sachadyn, P. (2017). Genome-wide DNA methylation profiling of the regenerative MRL/MpJ mouse and two normal strains. *Epigenomics*, *9*(8), 1105–1122. https://doi.org/10.2217/epi-2017-0009

Górnikiewicz, B., Ronowicz, A., Podolak, J., Madanecki, P., Stanislawska-Sachadyn, A., & Sachadyn, P. (2013). Epigenetic basis of regeneration: Analysis of genomic DNA methylation profiles in the MRL/MpJ mouse. *DNA Research*, *20*(6), 605–621. https://doi.org/10.1093/dnares/dst034

Herranz, M., Martín-Caballero, J., Fraga, M. F., Ruiz-Cabello, J., Flores, J. M., Desco, M., Marquez, V., & Esteller, M. (2006). The novel DNA methylation inhibitor zebularine is effective against the development of murine T-cell lymphoma. *Blood*, *107*(3), 1174–1177. https://doi.org/10.1182/blood-2005-05-2033

Ito, M., Yang, Z., Andl, T., Cui, C., Kim, N., Millar, S. E., & Cotsarelis, G. (2007). Wnt-dependent de novo hair follicle regeneration in adult mouse skin after wounding. *Nature*, *447*(7142), 316–320. https://doi.org/10.1038/nature05766

Kim, C. H., Marquez, V. E., Mao, D. T., Haines, D. R., & McCormack, J. J. (1986). Synthesis of pyrimidin-2-one nucleosides as acid-stable inhibitors of cytidine deaminase. *Journal of Medicinal Chemistry*, *29*(8), 1374–1380. https://doi.org/10.1021/jm00158a009

Langa, P., Wardowska, A., Zieliński, J., Podolak-Popinigis, J., Sass, P., Sosnowski, P., Kondej, K., Renkielska, A., Sachadyn, P., Pikula, M., & Trzonkowski, P. (2018). Transcriptional profile of in vitro expanded human epidermal progenitor cells for the treatment of non-healing

wounds. *Journal of Dermatological Science*, *89*(3), 272–281. https://doi.org/10.1016/j.jdermsci.2017.12.003

Lee, G., Wolff, E., & Miller, J. H. (2004). Mutagenicity of the cytidine analog zebularine in *Escherichia coli*. *DNA Repair*, *3*(2), 155–161. https://doi.org/10.1016/j.dnarep.2003.10.010

Marquez, V. E., Barchi, J. J., Kelley, J. A., Rao, K. V., Agbaria, R., Ben-Kasus, T., Cheng, J. C., Yoo, C. B., & Jones, P. A. (2005). Zebularine: A unique molecule for an epigenetically based strategy in cancer chemotherapy. The magic of its chemistry and biology. *Nucleosides, Nucleotides and Nucleic Acids*, *24*(5–7), 305–318. https://doi.org/10.1081/ncn-200059765

Marshall, C. D., Hu, M. S., Leavitt, T., Barnes, L. A., Lorenz, H. P., & Longaker, M. T. (2018). Cutaneous scarring: Basic science, current treatments, and future directions. *Advances in Wound Care*, *7*(2), 29–45. https://doi.org/10.1089/wound.2016.0696

Martinengo, L., Olsson, M., Bajpai, R., Soljak, M., Upton, Z., Schmidtchen, A., Car, J., & Järbrink, K. (2019). Prevalence of chronic wounds in the general population: Systematic review and meta-analysis of observational studies. *Annals of Epidemiology*, *29*, 8–15. https://doi.org/10.1016/j.annepidem.2018.10.005

McGowan, K. M., & Coulombe, P. A. (1998). Onset of keratin 17 expression coincides with the definition of major epithelial lineages during skin development. *The Journal of Cell Biology*, *143*(2), 469–486. https://doi.org/10.1083/jcb.143.2.469

Michaels, J., Churgin, S. S., Blechman, K. M., Greives, M. R., Aarabi, S., Galiano, R. D., & Gurtner, G. C. (2007). db/db mice exhibit severe wound-healing impairments compared with other murine diabetic strains in a silicone-splinted excisional wound model. *Wound Repair and Regeneration*, *15*(5), 665–670. https://doi.org/10.1111/j.1524-475x.2007.00273.x

Naldaiz-Gastesi, N., Bahri, O. A., Lopez de Munain, A., McCullagh, K. J., & Izeta, A. (2018). The panniculus carnosus muscle: An evolutionary enigma at the intersection of distinct research fields. *Journal of Anatomy*, *233*(3), 275–288. https://doi.org/10.1111/joa.12840

Nasir, N. J. M., Corrias, A., Heemskerk, H., Ang, E. T., Jenkins, J. H., Sebastin, S., & Tucker-Kellogg, L. (2022). The panniculus carnosus muscle: A missing link in the chronicity of heel pressure ulcers? *Journal of The Royal Society Interface*, *19*(187), 20210631. https://doi.org/10.1098/rsif.2021.0631

Nowak, N. C., Menichella, D. M., Miller, R., & Paller, A. S. (2021). Cutaneous innervation in impaired diabetic wound healing. *Translational Research*, *236*, 87–108. https://doi.org/10.1016/j.trsl.2021.05.003

Orta, M. L., Pastor, N., Burgos-Morón, E., Domínguez, I., Calderón-Montaño, J. M., Castaño, C. H., Lopez-Lazaro, M., Helleday, T., & Mateos, S. (2017). Zebularine induces replication-dependent double-strand breaks which are preferentially repaired by homologous recombination. *DNA Repair*, *57*, 116–124. https://doi.org/10.1016/j.dnarep.2017.07.002

Oyen, T., Votruba, I., Holy, A., & Wightman, R. (1973). Mechanism of inhibition of DNA synthesis in *Escherichia coli* by pyrimidin-2-one. *Biochimica et Biophysica Acta*, *324*(1), 14–23. https://doi.org/10.1016/0005-2787(73)90246-3

Podolak-Popinigis, J., Ronowicz, A., Dmochowska, M., Jakubiak, A., & Sachadyn, P. (2016). The methylome and transcriptome of fetal skin: Implications for scarless healing. *Epigenomics*, *8*(10), 1331–1345. https://doi.org/10.2217/epi-2016-0068

Reddy, S., Andl, T., Bagasra, A., Lu, M. M., Epstein, D. J., Morrisey, E. E., & Millar, S. E. (2001). Characterization of Wnt gene expression in developing and postnatal hair follicles and identification of Wnt5a as a target of Sonic hedgehog in hair follicle morphogenesis. *Mechanisms of Development*, *107*(1–2), 69–82. https://doi.org/10.1016/s0925-4773(01)00452-x

Reines, B., Cheng, L. I., & Matzinger, P. (2009). Unexpected regeneration in middle-aged mice. *Rejuvenation Research*, *12*(1), 45–52. https://doi.org/10.1089/rej.2008.0792

Sass, P., Sosnowski, P., Podolak-Popinigis, J., Górnikiewicz, B., Kamińska, J., Deptuła, M., Nowicka, E., Wardowska, A., Ruczynski, J., Rogujski, P., Filipowicz, N., Mieczkowska, A., Peszynska-Sularz, G., Janus, L., Skowron, P., Czupryn, A., Mucha, P., Piotrowski, A., & Rekowski, P. (2019). Epigenetic inhibitor zebularine activates ear pinna wound closure in the mouse. *EBioMedicine*, *46*, 317–329. https://doi.org/10.1016/j.ebiom.2019.07.010

Sawicka, J., Dzierżyńska, M., Wardowska, A., Deptuła, M., Rogujski, P., Sosnowski, P., Filipowicz, N., Mieczkowska, A., Sass, P., Hac, A., Schumacher, A., Gucwa, M., Karska, N., Kaminska, J., Platek, R., Mazuryk, J., Zielinski, J., Kondej, K., & Pawlik, A. (2020). Imunofan—RDKVYR peptide—Stimulates skin cell proliferation and promotes tissue repair. *Molecules*, *25*(12), 2884. https://doi.org/10.3390/molecules25122884

Schneider, C. A., Rasband, W. S., & Eliceiri, K. W. (2012). NIH Image to ImageJ: 25 years of image analysis. *Nature Methods*, *9*(7), 671–675. https://doi.org/10.1038/nmeth.2089

Seifert, A. W., Kiama, S. G., Seifert, M. G., Goheen, J. R., Palmer, T. M., & Maden, M. (2012). Skin shedding and tissue regeneration in African spiny mice (Acomys). *Nature*, *489*(7417), 561–565. https://doi.org/10.1038/nature11499

Votruba, I., Holý, A., & Wightman, R. (1973). The mechanism of inhibition of DNA synthesis in *Escherichia coli* by pyrimidin-2-one β-d-ribofuranoside. *Biochimica et Biophysica Acta (BBA) - Nucleic Acids and Protein Synthesis*, *324*(1), 14–23. https://doi.org/10.1016/0005-2787(73)90246-3

Wang, X., Ge, J., Tredget, E. E., & Wu, Y. (2013). The mouse excisional wound splinting model, including applications for stem cell transplantation. *Nature Protocols*, *8*(2), 302–309. https://doi.org/10.1038/nprot.2013.002

Williams-Boyce, P. K., & Daniel, J. C., Jr. (1980). Regeneration of rabbit ear tissue. *Journal of Experimental Zoology*, *212*(2), 243–253. https://doi.org/10.1002/jez.1402120211

Yus, E. S., & Simón, P. (2000). Striated muscle: A normal component of the dermis and subcutis in many areas of the face. *The American Journal of Dermatopathology*, *22*(6), 503–509. https://doi.org/10.1097/00000372-200012000-00004

Zhou, L., Cheng, X., Connolly, B., Dickman, M., Hurd, P., & Hornby, D. (2002). Zebularine: A novel DNA methylation inhibitor that forms a covalent complex with DNA methyltransferases. *Journal of Molecular Biology*, *321*(4), 591–599. https://doi.org/10.1016/s0022-2836(02)00676-9

## SUPPORTING INFORMATION

Additional supporting information can be found online in the Supporting Information section at the end of this article.

**How to cite this article:** Sass, P., Sosnowski, P., Kamińska, J., Deptuła, M., Skoniecka, A., Zieliński, J., Rodziewicz-Motowidło, S., Pikuła, M., & Sachadyn, P. (2022). Examination of epigenetic inhibitor zebularine in treatment of skin wounds in healthy and diabetic mice. *Journal of Tissue Engineering and Regenerative Medicine*, 1–11. https://doi.org/10.1002/term.3365